Cell Stem Cell
Article

In Vivo Mapping of Notch Pathway Activity in Normal and Stress Hematopoiesis

Philmo Oh,[1,7] Camille Lobry,[1,7] Jie Gao,[1] Anastasia Tikhonova,[1] Evangelia Loizou,[1] Jan Manent,[3] Ben van Handel,[4] Sherif Ibrahim,[2] Jeffrey Greve,[5,8] Hanna Mikkola,[4] Spyros Artavanis-Tsakonas,[3,6] and Iannis Aifantis[1,*]
[1]Howard Hughes Medical Institute and NYU Cancer Institute
[2]Department of Pathology and NYU Cancer Institute
New York University School of Medicine, New York, NY 10016, USA
[3]Department of Cell Biology, Harvard Medical School, Boston, MA 02115, USA
[4]Department of Molecular, Cell and Developmental Biology, Eli and Edythe Broad Stem Cell Research Center, University of California, Los Angeles, Los Angeles, CA 90095, USA
[5]Exelixis Inc., South San Francisco, CA 94080, USA
[6]Collège de France, 75231 Paris, Cedex 05, France
[7]These authors contributed equally to this work
[8]Present address: aTyr Pharma Inc., San Diego, CA 92121, USA
*Correspondence: iannis.aifantis@nyumc.org
http://dx.doi.org/10.1016/j.stem.2013.05.015

SUMMARY

Accumulating evidence suggests that Notch signaling is active at multiple points during hematopoiesis. Until recently, the majority of such studies focused on Notch signaling in lymphocyte differentiation and knowledge of individual Notch receptor roles has been limited due to a paucity of genetic tools available. In this manuscript we generate and describe animal models to identify and fate-map stem and progenitor cells expressing each Notch receptor, delineate Notch pathway activation, and perform in vivo gain- and loss-of-function studies dissecting Notch signaling in early hematopoiesis. These models provide comprehensive genetic maps of lineage-specific Notch receptor expression and activation in hematopoietic stem and progenitor cells. Moreover, they establish a previously unknown role for Notch signaling in the commitment of blood progenitors toward the erythrocytic lineage and link Notch signaling to optimal organismal response to stress erythropoiesis.

INTRODUCTION

Notch signaling defines a conserved, fundamental pathway responsible for determination in metazoan development and is widely recognized as an essential component of lineage-specific differentiation and stem cell self-renewal in many tissues (Artavanis-Tsakonas et al., 1995; Kopan and Ilagan, 2009), including the hematopoietic system. Hematopoiesis is a complex process that requires coordination between proliferation, self-renewal, and differentiation of stem and progenitor cells to generate mature blood cells (Orkin and Zon, 2008). All Notch receptor paralogs (Notch1–4) and their ligands have been implicated in the regulation of diverse functions in the hematopoietic system. The best-described functions of Notch are in the emergence of fetal hematopoietic stem cells (HSCs) (Clements et al., 2011; Dzierzak and Speck, 2008; Kumano et al., 2003) and T cell commitment and early development. Indeed, the significance of Notch1 for T lymphocyte commitment, differentiation, and oncogenic transformation has been well established (Ciofani and Zúñiga-Pflücker, 2005; Grabher et al., 2006; Tanigaki et al., 2002). Recent studies have also suggested a function for Notch in hematopoietic regeneration (Butler et al., 2010; Varnum-Finney et al., 2011); however, its relevance for the self-renewal and maintenance of adult HSCs has been questioned (Maillard et al., 2008).

On the other hand, data regarding its involvement in nonlymphoid adult blood lineages is scarce and often controversial. Recent studies suggested a role for Notch4 in megakaryocyte (Mk) differentiation (Mercher et al., 2008), but further studies in human hematopoietic progenitors challenged this conclusion (Poirault-Chassac et al., 2010). Furthermore, there is little evidence connecting specific Notch receptors with nonlymphoid hematopoietic lineages. We recently reported that the conditional silencing of Notch signaling in the bone marrow results in the expansion of granulocyte-monocyte progenitors (GMPs) and that eventually these animals develop a chronic myelomonocytic leukemia (CMML)-like disease (Klinakis et al., 2011), suggesting that Notch signaling might be involved in early stem/progenitor cell fate decisions.

To fate-map Notch receptor expression and pathway activity in the hematopoietic system, we used tamoxifen-inducible CreER knockin mice for individual Notch receptors in combination with a Notch reporter strain (Hes1^{GFP}). Our lineage tracing studies have revealed an intriguing division of labor between *Notch1* and *Notch2*, with the former marking mainly lymphocyte progenitors and the latter reaching peak levels during early erythropoiesis. Interestingly, *Hes1*- or *Notch2*-expressing progenitors were enriched for erythroid potential and upregulated the expression of an erythroid gene program. Accordingly, conditional Notch gain-of-function in hematopoietic progenitors promoted erythroid commitment and Notch loss-of-function decreased the number of erythroid progenitors and increased

peripheral blood platelet counts. Using a combination of genetic fate mapping, transgenic reporters, and conditional Notch gain-/loss-of-function, we define lineages regulated by individual Notch receptors and reveal a role for Notch signaling in physiological and stress erythropoiesis.

RESULTS

Notch Receptor In Vivo Lineage Tracing Reveals a Division of Labor during Early Hematopoiesis

To lineage-trace Notch receptor expression in hematopoiesis, we have used mice with the CreER^{T2} cassette knocked into the endogenous loci of each of the Notch receptors. We crossed them to the *ROSA26*$^{lsl\text{-}RFP}$ reporter strain (Luche et al., 2007) (Figure 1A). After receiving tamoxifen and after various periods of chase, *Notch(1–4)*^{CreER} mice were analyzed, and only *Notch1* and *Notch2* were detectable in bone marrow progenitors. After both 3 and 7 day chase, *Notch1*^{CreER} predominantly labeled bone marrow progenitors with lymphoid potential, including lymphoid-primed multipotent progenitors (L-MPPs) and common lymphoid progenitors (CLPs) (Figures 1B–1D and Figures S1A and S1B available online). In contrast, *Notch2*^{CreER}-labeled cells were found mostly in nonlymphoid progenitors, indicating that there is lineage-specific expression of Notch receptors in stem/progenitor cells. The peaks of *Notch2* labeling were within the HSC and pre-erythrocytic stages of differentiation. Interestingly, short chase labeling experiments indicated an almost complete absence of *Notch1* labeling within all nonlymphoid progenitor subsets, likely reflecting the lack of receptor expression of *Notch1* in all such subsets. Intriguingly, even after 20 weeks of chase, there were sustained higher levels of *Notch2* labeling within the myelo-erythroid fraction (Figures S1C and S1D).

Closer analysis of progenitor subsets in *Notch2*^{CreER} mice revealed that the percentage of RFP$^+$ cells was significantly higher in erythroid and megakaryocytic progenitors (pre-megakaryocyte-erythrocytes [pre-MegEs], colony forming unit erythrocytes [CFU-Es], and megakaryocyte progenitors [MkPs]) than in GMPs at both 3 and 7 days after tamoxifen injection. After a 3 day chase, approximately 15% and 30% of pre-MegEs and CFU-Es, respectively, were RFP$^+$ compared to 2% in the GMP subset (Figure 1B). This implied that expression of *Notch2* could be important in the megakaryocyte-erythrocyte (MegE) versus granulocyte-monocyte (GM) cell fate decision at an early progenitor stage. Additionally, *Notch2*^{CreER}-labeled cells were found with increasing frequency within the erythroid progenitor fraction (up to 35%) in comparison to MkPs (<10%) (Figures 1B and 1D). From the bipotent pre-MegE to the CFU-E erythroid progenitor, there was a sustained increase in RFP$^+$ cells, whereas the frequency actually decreased between the pre-MegE and the MkP at both time points. *Notch3* and *Notch4* labeling was not detected in the bone marrow (Figures 1B and 1D). *Notch3* labeling appeared in early thymic T cell progenitors and was detectable in mature T cells with longer periods of chase (Figure 1C and data not shown). *Notch4* labeling was extremely infrequent throughout the hematopoietic system but was detectable in splenic CD8$^+$CD11c$^+$ dendritic cells (DCs), in agreement with previous quantitative RT-PCR data (Sekine et al., 2009) (Figure S1F). To confirm lineage tracing results at the level of transcription, we carried quantitative RT-PCR analysis for the four Notch receptors (Figure S1E). Similar to our lineage tracing results, mainly *Notch2* mRNA was detected in HSCs, with only low levels of *Notch1* mRNA. In the myelo-erythroid progenitor compartment, *Notch1* was detected at low levels in GMPs and pre-MegEs, whereas *Notch2* was detected at significantly higher levels. Only *Notch2* mRNA was detected in CFU-Es and MkPs. Consistently, no expression of *Notch3* and *Notch4* mRNA was detected in these populations.

Furthermore, we were able to confirm these fate-mapping studies using receptor-specific antibodies (Fiorini et al., 2009). Indeed, Notch1 surface labeling increased during commitment to the lymphocytic lineage and did not appear to be detectable outside the lymphoid lineage. Conversely, Notch2 was not expressed in early lymphoid progenitors (Figure 1E). Expression of Notch2 was low in CMPs and GMPs but significantly higher in erythroid progenitors (pre-MegEs, CFU-Es, and proerythroblasts [ProEs]). Notch2 surface labeling reached a peak in CFU-E progenitors and proerythroblasts but began to decrease at the basophilic erythroblast stage (Figure 1E and data not shown). In comparison to erythroid progenitors, MkPs expressed lower levels of surface Notch2. Whereas only a fraction of cells from populations like HSCs were stained in the lineage tracing experiments, most of these cells appeared to be stained using antibodies. This discrepancy most likely reflects a partial recombination efficiency of CreER, particularly after limited numbers of tamoxifen injections. Consistent with the lineage tracing results, Notch4 surface expression was detectable in a subset of splenic DCs (Figure S1G) and undetectable in hematopoietic stem and progenitor cells (HSPCs) in the bone marrow (Figure S1H), once more suggesting that Notch4 signaling plays no role during early hematopoiesis. Our combined lineage tracing and antibody labeling studies suggested a very tightly regulated division of labor between the Notch1 and Notch2 receptors during early stages of hematopoiesis.

In Vivo Mapping of Notch Pathway Activation during Early Hematopoiesis

To combine lineage tracing and receptor expression with pathway activation, we used a reporter knockin allele (Fre et al., 2011) in which the *Hes1* locus, a well-known direct transcriptional target of Notch, drives expression of GFP (Hirata et al., 2002; Ntziachristos et al., 2012) (Figure 2A). To validate the model, we initially characterized the thymus, where the role of *Notch1* is well established. We found that *Hes1* mRNA expression was more than 50-fold higher in cells expressing *Hes1*^{GFP} and that expression of other well-characterized Notch target genes was also increased in *Hes1*$^{GFP+}$ cells, confirming that *Hes1*-expressing cells reflected the activation of the Notch pathway (Figure S2A). In the thymus, *Hes1*^{GFP} expression was first detected in a fraction of early T cell progenitors (ETPs) and increased during T cell commitment up to the DN3 (CD4$^-$CD8$^-$CD25$^+$cKit$^-$CD44$^-$) stage where Notch activation reached its peak (Figures S2B and S2C). After this stage of differentiation, Notch signaling activity is downregulated (Kleinmann et al., 2008). Accordingly, we found that in CD4$^+$CD8$^+$ double positive T cells (DPs), the expression of *Hes1*^{GFP} was also downregulated (Figures S2B and S2C). Consistent with this differentiation and stage-specific *Hes1* expression, GFP$^+$ cells were

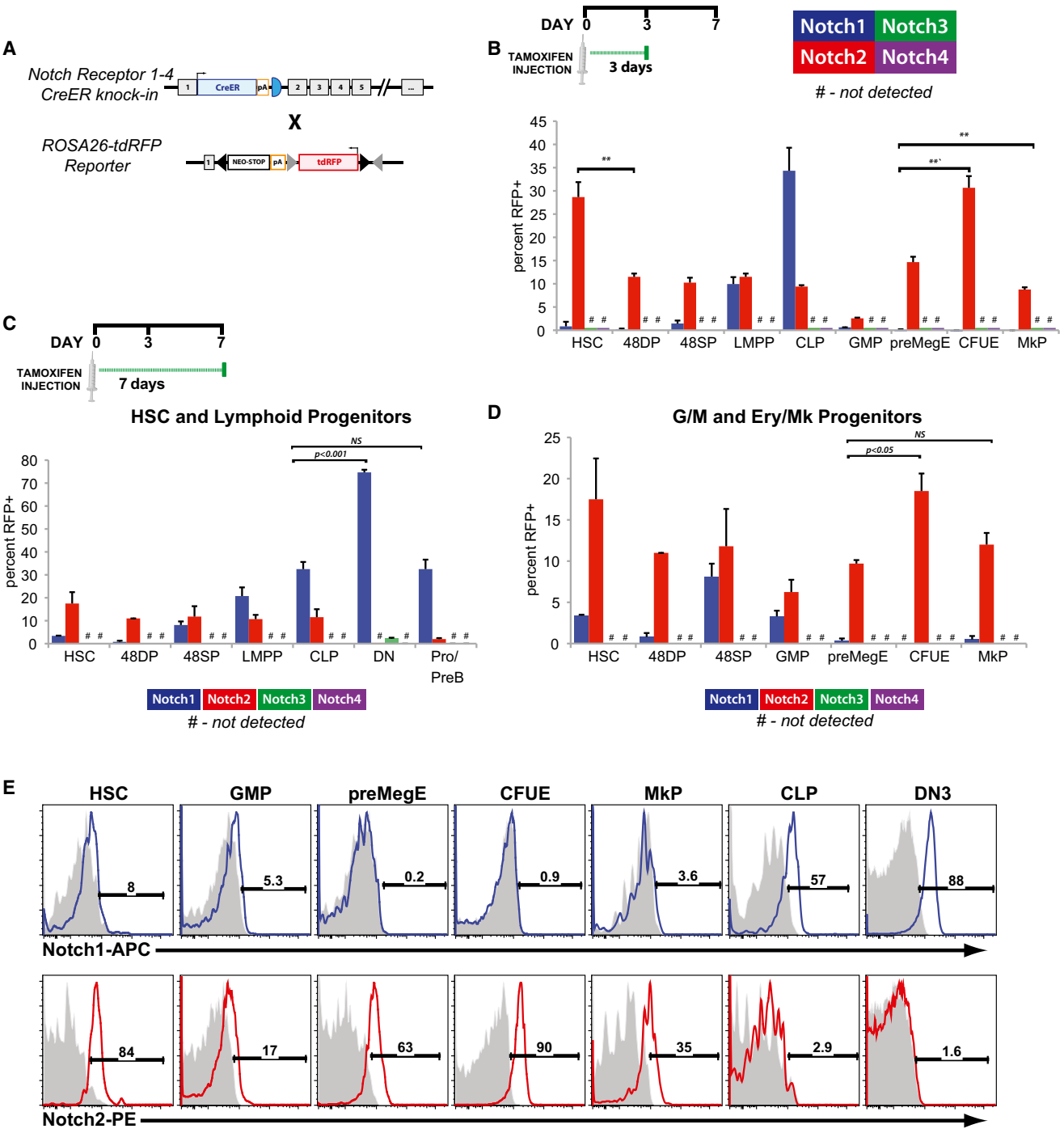

Figure 1. *Notch(1–4)*^{CreER} In Vivo Lineage Tracing Suggests a Division of Labor between Notch1 and Notch2 during Early Adult Hematopoiesis

(A) Schematic depiction of the Notch(1–4)^{CreER} × ROSA26^{RFP} mouse strain.

(B) Analysis of RFP reporter expression 72 hrs after a single injection of tamoxifen focused at defined stem and progenitors populations. Frequency of reporter labeling is represented as mean ± standard deviation (SD) (n = 5 for each cohort).

(C and D) Analysis of RFP reporter expression in LT-HSCs, lymphoid progenitors, and granulocyte/monocyte (G/M) and erythrocyte-megakaryocyte (Ery/Mk) progenitor subsets 1 week after a single tamoxifen injection (n = 5). Bars denote mean ± SD.

(E) Antibody staining with APC-conjugated anti-Notch1 and PE-conjugated anti-Notch2. Notch1 expression (blue histograms) and Notch2 (red histograms) are overlaid on isotype controls (gray filled histograms) for the same population. *p < 0.05, **p < 0.005.

HSC, Lin^{neg}/cKit^{+}/Sca1^{+}/Flt3^{-}/CD48^{-}/CD150^{+}; 48DP, Lin^{neg}/cKit^{+}/Sca1^{+}/Flt3^{-}/CD48^{+}/CD150^{+}; 48SP, Lin^{neg}/cKit^{+}/Sca1^{+}/Flt3^{-}/CD48^{+}/CD150^{-}; LMPP, Lin^{neg}/cKit^{+}/Sca1^{+}/Flt3^{+}/IL7rα^{-}; CLP, Lin^{neg}/cKit^{lo}/Sca1^{lo}/Flt3^{+}/IL7rα^{+}; GMP, Lin^{neg}/cKit^{+}/Sca1^{-}/CD41^{-}/CD150^{-}/FcgRII/III^{+}; pre-MegE, Lin^{neg}/cKit^{+}/Sca1^{-}/CD41^{-}/FcγRII/III^{-}/CD150^{+}/CD105^{-}; CFU-E, Lin^{neg}/cKit^{+}/Sca1^{-}/CD41^{-}/FcγRII/III^{-}/CD150^{-}/CD105^{+}; MkP, Lin^{neg}/cKit^{+}/Sca1^{-}/CD41^{+}/CD150^{+}; DN3, CD4^{-}/CD8^{-}/CD44^{-}/cKit^{-}/CD25^{+}; and pro/preB, B220^{+}/IgM^{-}. See also Figure S1.

located primarily in the thymic cortex (Figure S2D). These studies validated the use of the *HES1*^{GFP} mice as a faithful Notch reporter in the immune system. In agreement with this idea, high levels of *Hes1* expression were also found in marginal zone B cells (MZBs), which require Notch signaling (Moriyama et al., 2008; Tanigaki et al., 2002; data not shown).

Notch Pathway Activation Marks Initiation of Commitment to the Erythroid Lineage

In the bone marrow, *Hes1*^{GFP} expression was detected within the Lin^{neg}cKit^{+} hematopoietic fraction containing stem and progenitor cells. Interestingly, *Hes1* expression was detected within the LT-HSC fraction and was virtually undetectable at the downstream multipotential progenitor (MPP) subsets (Figure 2B). Whole-transcriptome studies of both *Hes1*^{GFP}-positive and -negative Lin^{neg}/cKit^{+}/Sca1^{+} (LSK) cells supported our phenotypic analysis because they correlated the Hes1^{GFP} fraction to the expression of genes, characteristic of the HSC stage (Figure S3A). Interestingly, *Hes1*^{GFP} LSK cells also expressed gene signatures correlating to erythrocytic differentiation, suggesting an early molecular bias toward the erythrocytic and against the GM/Mk lineages (Figures S3B and S3C). Further fractionation of long-term HSCs (LT-HSCs) based on their GFP expression showed that the observed erythroid bias seen at the level of LSK population was also evident in this compartment. Indeed, LT-HSCs expressed higher levels of key erythroid genes such as *Klf1* or *Epor* and lower levels of myelo/lymphoid genes such as *Sfpi1* (Figure S3D). Furthermore, when LSK GFP^{+} and GFP^{-} were tested for their erythroid potential in methylcellulose CFU-E colony assay, LSK cells expressing *Hes1* showed greater erythroid colony forming potential (Figure S3E). In agreement with this expression profiling and our aforementioned lineage tracing experiments, which demonstrated an erythroid bias in *Notch2*^{CreER} labeling, *Hes1* expression was virtually undetectable at the CMP and GMP subsets (Figure S2E) and significantly derepressed at the bipotent pre-MegE stage and subsequently increased as cells committed to the erythroid lineage, at the pre-CFU-E and CFU-E stages (Figure 2C). The extent of Notch activation was more pronounced in the spleen, a major site of erythrocytic differentiation in the mouse, because high levels of *Hes1*^{GFP} were detected in erythrocytic progenitors (Figures 2D and 2E). This higher pathway activity in the spleen could not be explained by differential surface expression of Notch2 and most likely reflects differential ligand availability in this tissue (data not shown). Interestingly, the activation of the Notch pathway was transient in both tissues as it was downregulated at later stages of erythrocytic differentiation (Figure S2F). *Hes1* expression remained low in MkPs, suggesting that Notch is not active (or is attenuated) in early Mk development (Figure S2G).

To directly connect *Hes1*^{GFP} expression to Notch signaling we have crossed the *Hes1*^{GFP} mice to animals that conditionally lack gamma-secretase activity and thus Notch signaling (*Vav1-cre Ncstn*$^{f/f}$). We had previously shown that *Ncstn* deletion phenocopies Notch receptor loss and that *Ncstn*$^{-/-}$ phenotypes could be rescued totally by the expression of an activated form of Notch (Klinakis et al., 2011). Using *Vav1-cre Ncstn*$^{f/f}$ *Hes1*^{GFP} mice, we were able to show that Notch inactivation led to an almost complete reduction of *Hes1*^{GFP} levels in erythrocyte progenitors, suggesting direct regulation of *Hes1* expression by Notch signaling in erythrocytic progenitors (Figures 2F and 2G).

Differential Patterns of Notch Activity between Fetal and Adult Hematopoiesis

Because initiation of erythropoiesis is a crucial event during fetal hematopoiesis, we decided to study the activation of Notch signaling and its relationship to red blood cell differentiation in the embryo. We first looked at primitive hematopoiesis in the yolk sac. We carried quantitative RT-PCR for each of the Notch receptors as well as for *Hes1*. Yolk sac HSPCs expressed both *Notch1* and *Notch2* but showed no *Hes1* expression, suggesting that Notch signaling is not activated at this stage. Interestingly, Mks and red blood cells showed only expression of *Notch2* and red blood cells also expressed moderate but significant levels of *Hes1*, suggesting activation of the Notch pathway (Figures S3F and S3G). We then focused on fetal liver embryonic hematopoiesis. We probed Notch receptor expression by RT-PCR and found mainly *Notch2* expression (Figure 3A). *Notch1* had low expression levels in HSCs, CMPs, and GMPs but was not expressed in megakaryocyte/erythrocyte progenitors (MEPs), consistent with our observation in adult stem and progenitor cells. We then used the *Hes1*^{GFP} reporter strain to probe activation of the Notch pathway. Interestingly, we found that fetal liver hematopoiesis follows a pattern of activation distinct from what we reported in adults. At embryonic day 13.5, the majority of the phenotypic LT-HSCs expressed significant amounts of *Hes1*, but this expression was absent from more committed progenitors (Figure 3B). *Hes1*$^{GFP+}$ HSCs were bona fide LT-HSCs capable of long-term full lineage reconstitution of lethally irradiated recipients (data not shown). Similar to sorted *Hes1*^{GFP} cells from adult mice, fetal liver HSCs expressing *Hes1* were characterized by a Notch transcriptional signature (Figures 3C and 3D), as judged by transcriptome profiling and quantitative RT-PCR studies. Interestingly, *Hes1*^{GFP}-expressing fetal HSCs also revealed a lymphocytic gene expression bias, in contrast to the erythroid bias found in adult *Hes1*^{GFP}-expressing HSCs (Figures 3D and 3E). Furthermore, *Hes1* expression and Notch pathway activation was undetectable in fetal erythroid progenitors, underlining the differences between fetal and adult hematopoiesis in regard to Notch activation.

Hes1^{+} Progenitors Show Increased Erythroid Potential and an Erythroid Transcriptional Profile

Next, we returned to adult hematopoiesis and further focused on the connection of Notch activity to erythropoiesis. Lin^{neg}/cKit^{+}/Sca1^{-} progenitors (cKit^{+} progenitors) were sorted based on *Hes1*^{GFP} expression and plated into methylcellulose or collagen-based semisolid medium to be assayed for lineage potential. *Hes1* expressing cells were enriched in the erythroid lineage potential whereas *Hes1*-negative mainly differentiated into granulocytes/monocytes (GMs) or Mks (Figure 4A). FACS analysis demonstrated Gr1^{+}CD11b^{+} cells were virtually absent in colonies generated by Hes1^{+} progenitors and that most cells expressed the erythroid marker TER-119. This enhancement in erythroid potential was supported by CFU-E assays, which confirmed this striking difference in the presence of Hes1 expression (Figure 4B). In addition, there were fewer CD41^{+} cells in colonies from Hes1^{+} progenitors (Figure 4A). We further

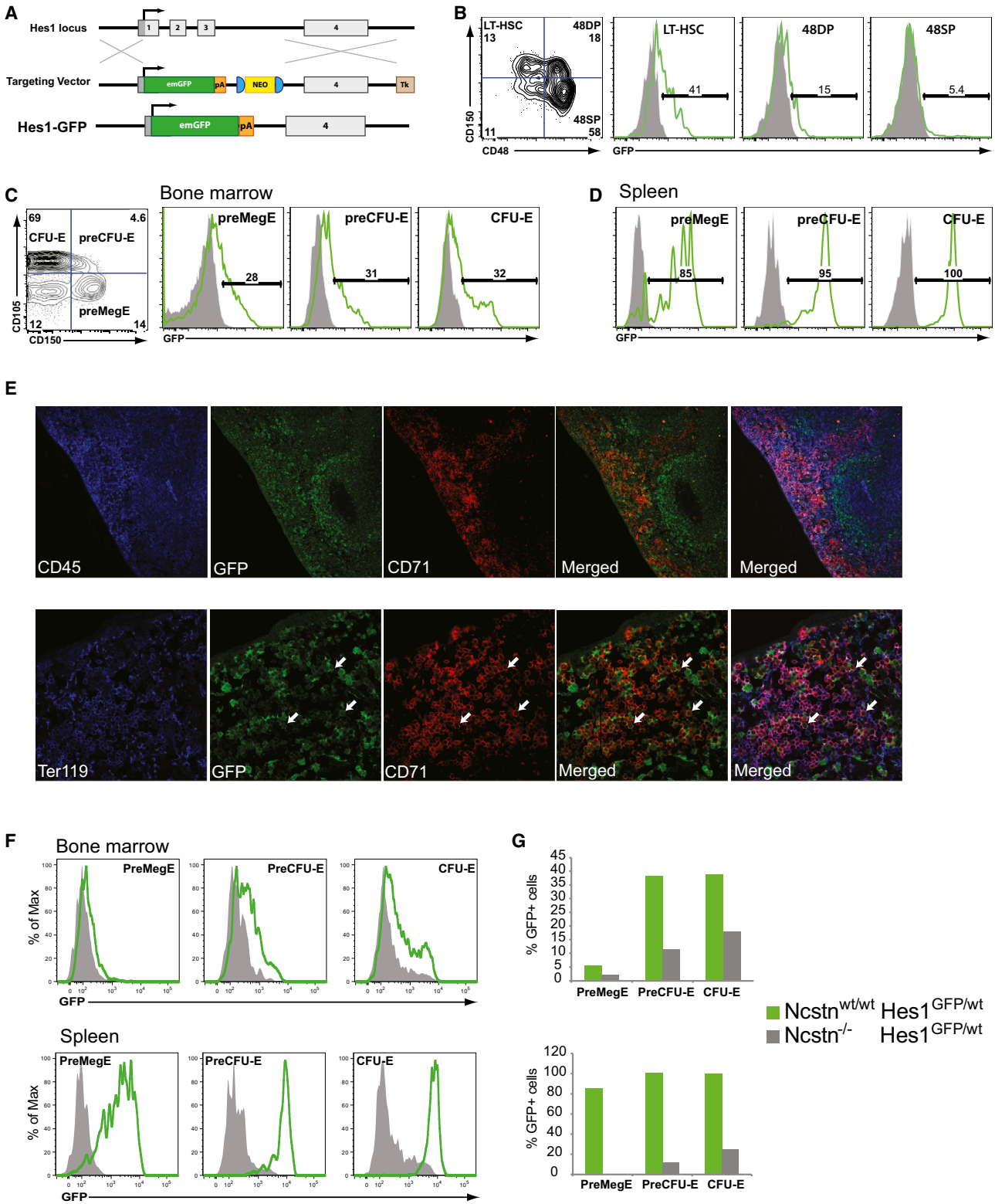

Figure 2. The *Hes1*^{GFP} Reporter Identifies Points of Notch Pathway Activity

(A) Targeting strategy used to express GFP from the endogenous *Hes1* promoter.

(B) Analysis of LSK stem and progenitor cells in bone marrow of Hes1^{GFP} reporter mice.

(C and D) High-resolution separation of Lin^{neg}/cKit^{+}/Sca1^{-} progenitors on the basis of CD105, CD150, CD16/32 (FcγRII/III), and CD41 expression and expression of *Hes1*^{GFP} in erythroid progenitors in (C) bone marrow and (D) spleen (a representative of more than five experiments is shown).

(legend continued on next page)

addressed the Mk potential of cKit$^+$ progenitors in acetylcholinesterase (AchE)-stained collagen-based semisolid cultures, which is the definitive way to measure CFU-Mk potential (Jackson, 1973). *Hes1*$^+$ cells formed significantly fewer AchE$^+$ Mk colonies than *Hes1*^{neg} cells (Figure 4C). Furthermore, the infrequent CFU-Mk colonies generated by *Hes1*$^+$ progenitors were usually much smaller than CFU-Mk colonies from cells that were *Hes1*^{neg} (data not shown). The absence of a correlation between Notch activation and promotion of the Mk lineage further questions involvement of Notch4 signaling in this lineage commitment as previously suggested (Mercher et al., 2008).

To analyze the transcriptional program of progenitors with an active Notch pathway, we sorted cKit$^+$ progenitors based on expression level of *Hes1*^{GFP} and used them for whole-transcriptome analysis. Cluster analysis of microarrays from *Hes1*^{GFP} mice revealed that *Hes1*$^+$ progenitors have a transcriptional profile almost identical to pre-CFU-E erythroid progenitors (Pronk et al., 2007), whereas *Hes1*^{neg} progenitors clustered closely with pre-GM and MkP populations (Figure 4D). Also, we compiled genes important in erythroid, GM, and Mk lineage-specific differentiation and found that essential erythroid and Notch target genes were both upregulated in *Hes1*$^+$ progenitors (Figure 4E). The expression of GM and Mk-specific genes was downregulated. Changes in expression of selected genes were verified by quantitative RT-PCR. As expected, in the *Hes1*$^{GFP+}$ cells, *Hes1* and *Nrarp* expression was significantly upregulated, as was the expression of erythroid genes (*Epor* and *Gypa*) (Figure 4E and Figure S4A). The transcription factor *Runx1* and the thrombopoietin receptor *Mpl* are essential for generation of normal Mks and platelets. In GFP$^+$ progenitors, expression of both *Runx1* and *Mpl* was decreased compared to GFP$^-$. Moreover, the expression levels of transcription factors known to be important in the GM lineage, such as *Pu.1* (*Sfpi1*) and *Cebpa*, were reduced in GFP$^+$ progenitors (Figure 4E and Figure S4A).

To further compare the gene expression profiles of *Hes1*$^+$ to *Hes1*^{neg} Lin^{neg}cKit$^+$ progenitors, we used gene set enrichment analysis (GSEA) and analyzed expression of established lineage-affiliated gene sets by comparing the transcriptional profile of HSCs to more committed progenitors such as LMPPs, GMPs, and MEPs (Ng et al., 2009). Genetic signatures expressed in early (*s-ery*) and more committed (*d-ery*) erythroid progenitors were significantly enriched in *Hes1*$^+$ Lin^{neg}cKit$^+$ cells. In contrast, gene sets characteristic of GM and lymphoid progenitors (*r-myly*) showed a negative enrichment (Figure S4B). As previously mentioned, our microarray analysis indicated that key Mk-associated genes were repressed in *Hes1*$^+$ progenitors. Notably, using similar gene sets (Mercher et al., 2008) we revealed an inverse relationship between the expression of *Hes1* and Mk-related genes. Transcriptional profiling therefore supports the notion that *Hes1* expression is characteristic of progenitors committed (or destined to commit) to the erythroid lineage.

To probe the role of Notch signaling in human erythropoiesis, we examined public gene expression databases for expression of Notch-related genes. In agreement with the results presented thus far, we found, using meta-analysis of whole-transcriptome data (Novershtern et al., 2011), that Notch pathway genes were upregulated during human erythroid differentiation (Figure S4E). More importantly, expression of Notch direct transcriptional targets (including *Hes1, Hey1*, *Gata3*, and *Tcf7*) increased in human erythroid progenitors. We therefore propose that Notch activation is an evolutionarily conserved hallmark of erythroid differentiation not only in mice but also in humans, suggesting that our findings may be of broader significance.

Notch2 Signaling Commits Bipotent Pre-MegE Progenitors to the Erythroid Lineage

The bipotent pre-MegE progenitors generate erythroid and Mk progenitors both in vitro and in vivo (Pronk et al., 2007). To investigate whether Notch signaling can function at this branch point, we sorted pre-MegEs based on *Hes1*^{GFP} expression and plated cells in semisolid media. *Hes1*$^+$ cells generated a significantly higher number of pure erythroid colonies and fewer mixed erythroid-Mk colonies or pure Mk colonies (Figure 4F). Conversely, *Hes1*^{neg} pre-MegEs developed more mixed MegE colonies and pure Mk colonies. This suggested that in the absence of Notch signaling, pre-MegEs retain megakaryocytic potential. Also, in CFU-E assays, pre-MegEs that expressed *Hes1* generated more CFU-Es than the *Hes1*^{neg} ones (Figure 4G). We then focused on Notch2, as it is the only Notch receptor expressed on pre-MegE progenitors and the downstream early erythroid precursors (Figure 1, Figure S1). In agreement with our previous findings, pre-MegEs sorted for surface Notch2 expression generated more CFU-E erythroid colonies than Notch2^{low} progenitors (Figure S4C). Finally, GSEA of pre-MegEs, sorted based on *Hes1*^{GFP} expression, demonstrated that erythroid genes are enriched in the *Hes1*-expressing fraction in comparison to the GFP$^-$ fraction. Analysis of Mk transcription gene sets (Mercher et al., 2008) revealed an inverse relationship between the expression of *Hes1* and Mk-related genes as we previously found with cKit$^+$ progenitors (Figure S4D).

Notch2 Gain of Function Promotes Early Erythroid Progenitor Differentiation in Vivo

If Notch signaling activation characterizes commitment of adult hematopoietic progenitors to the erythrocytic lineage, it is conceivable that genetic manipulation of the pathway could promote or impede adult erythropoiesis in vivo. We thus generated transgenic mice expressing the active domain of each Notch receptor from the ubiquitously expressed ROSA26 promoter (Figure 5A). Using these animals, we conditionally expressed intracellular Notch-IC(1–4) (ICN1–4) using inducible Cre-recombinase strains and monitored expression of the transgene using YFP (Kühn et al., 1995; Ruzankina et al., 2007; Seibler et al., 2003). This approach allowed us to compare the functional

(E) Immunofluorescence staining of spleen from *Hes1*^{GFP} reporter mouse showing colocalization of GFP and CD71 staining in the red pulp.
(F) Representative histograms showing GFP levels in erythroid progenitors in bone marrow (upper panel) and spleen (lower panel) of *Ncstn*$^{wt/wt}$ *Hes1*$^{wt/GFP}$ and *Ncstn*$^{-/-}$ *Hes1*$^{wt/GFP}$.
(G) Bar graphs representing average percentage of GFP$^+$ cells in displayed populations from bone marrow (upper panel) and spleen (lower panel).
See also Figure S2.

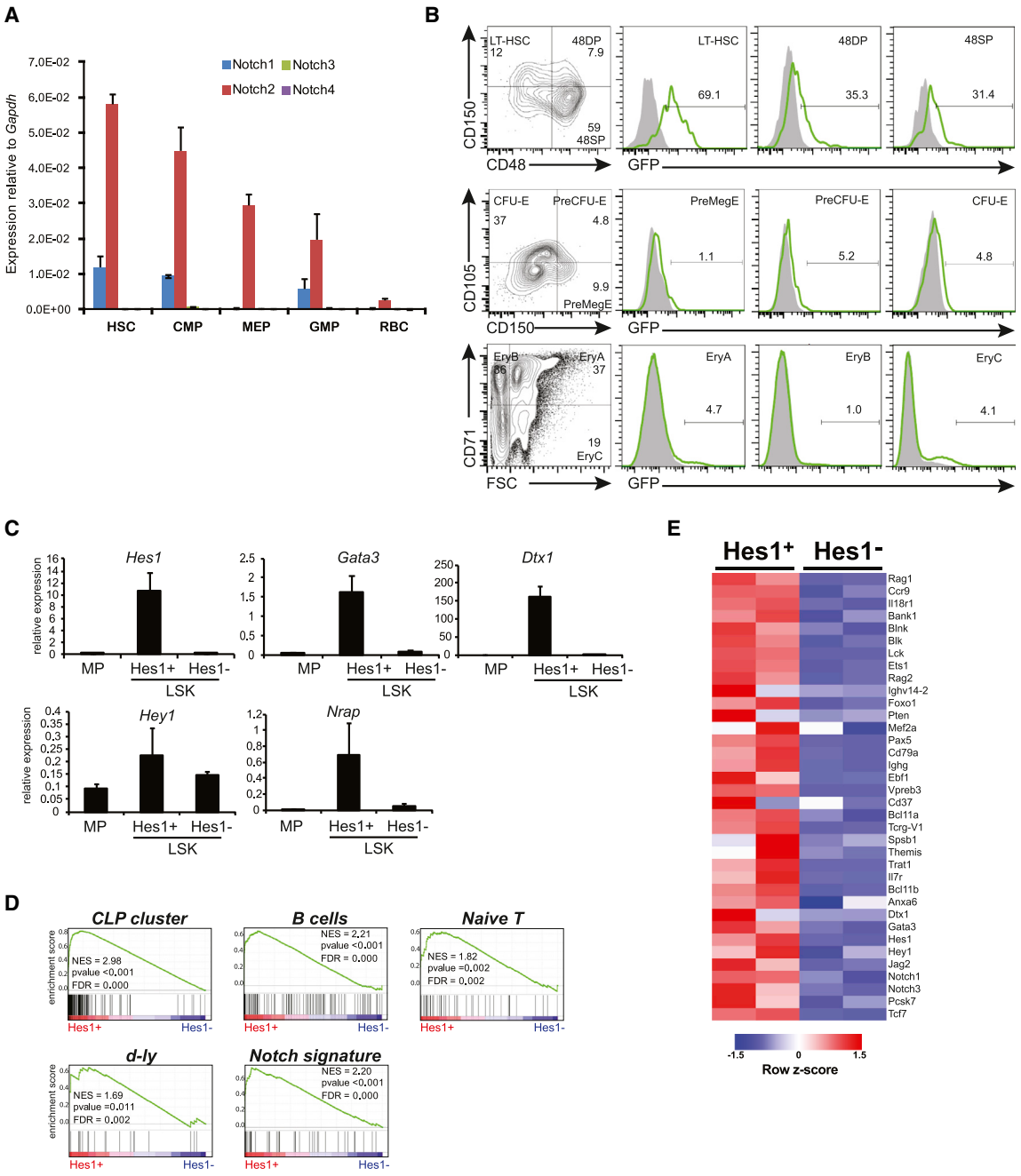

Figure 3. Differential Patterns of Notch Activity between Fetal and Adult Hematopoiesis

(A) Quantitative RT-PCR analysis of Notch receptor genes in Lin^{neg}/cKit^{+}/Sca1^{+}/CD48^{-}/CD150^{+} HSCs, Lin^{neg}/cKit^{+}/Sca1^{-}/CD34$^{+/}$FcgRII/III^{lo} CMPs, Lin^{neg}/cKit^{+}/Sca1^{-}/CD34^{-}/FcgRII/III^{-} MEPs, Lin^{neg}/cKit^{+}/Sca1^{-}/CD34$^{+/}$FcgRII/III^{hi} GMPs, and CD71+/ TER-119^{+} RBCs from E13.5 fetal liver. Data represent mean ± SD of three biological replicates.

(B) Expression of *Hes1^{GFP}* in fetal liver Lin^{neg}/cKit^{+}/Sca1^{+} stem and multipotential progenitor populations separated into LT-HSCs (CD48^{-}/CD150^{+}), CD48^{+}/CD150^{+} double positive cells (CD48DP), and CD48^{+}/CD150^{-} single positive cells (CD48SP) (upper panel) and in Lin^{neg}/cKit^{+}/Sca1^{-}/CD41^{-}/FcgRII/III^{-} pre-MegEs (CD150+/CD105−), pre-CFU-Es (CD150+/CD105+), and CFU-Es (CD150−/CD105+) (middle panel) and late erythrocyte progenitors (lower panel).

(C) Quantitative RT-PCR analysis of Notch signaling pathway target genes in Lin^{neg}/cKit^{+}/Sca1^{-} progenitors (MP) and Lin^{neg}/cKit^{+}/Sca1^{+} (LSK) GFP^{+} and GFP^{-} cells from E13.5 fetal liver. Data represent mean ± SD of three biological replicates.

(D) Gene set enrichment plots of fractionated Lin^{neg}/cKit^{+}/Sca1^{+} GFP^{+} versus GFP^{-} from E13.5 fetal liver of *Hes1^{GFP}* mice for the indicated gene sets.

(E) Heat map of lymphoid differentiation genes and Notch signaling pathway target genes expressed in Lin^{neg}/cKit^{+}/Sca1^{+} GFP^{+} versus GFP^{-} from E13.5 fetal liver.

See also Figure S3.

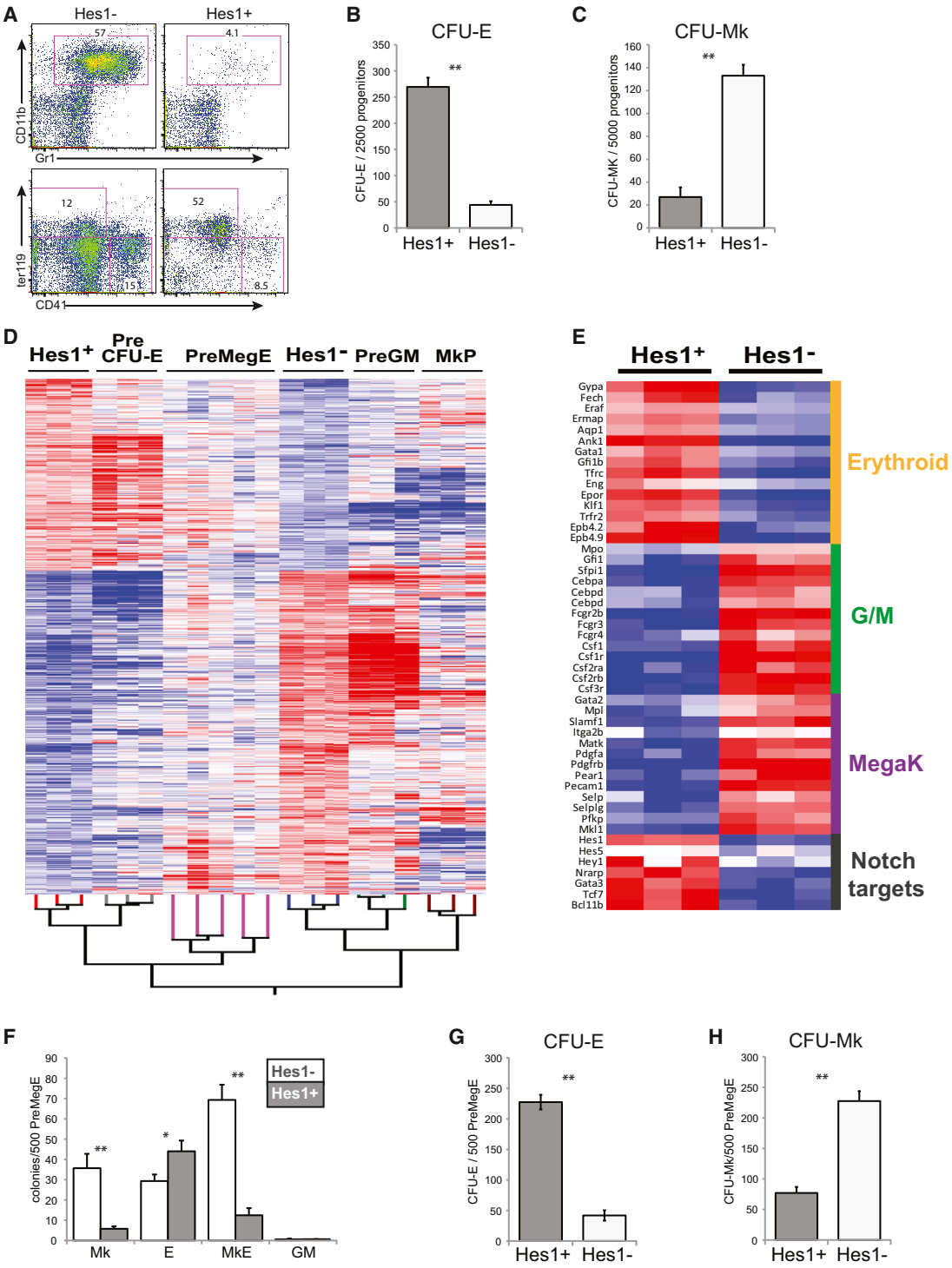

Figure 4. *Hes1* Expression and Notch Activity Are Predictive of Commitment to the Erythrocytic Lineage

(A) One week after methylcellulose culture in a complete cocktail of cytokines, colonies from *Hes1*-expressing (right panels) and *Hes1* negative $Lin^{neg}/cKit^{+}/Sca1^{-}$ progenitors (left panels) were analyzed by FACS for expression of Gr1 versus CD11b and TER-119 versus CD41. (B) CFU-E in methylcellulose supplemented with EPO and (C) CFU-Mk assays in collagen gel with TPO and IL-3 and sorted $Lin^{neg}/cKit^{+}/Sca1^{-}$ progenitors from $Hes1^{GFP}$ bone marrow. (D) Hierarchical clustering of fractionated $Hes1^{GFP}$ $Lin^{neg}/cKit^{+/}Sca1^{-}$ progenitors with other progenitor populations. (E) Heat map of Notch target genes and key genes expressed in the erythroid, granulocyte/monocyte (G/M), and megakaryocyte (MegaK) lineages. Bars denote standard deviation. (F) Lineage potential of sorted pre-MegE progenitors was evaluated in complete methylcellulose 7 days after sorting. (G) CFU-E assay and (H) CFU-Mk assay of sorted pre-MegEs based on *Hes1* expression ($Hes1^{+}$, dark gray bar; $Hes1^{-}$, light gray bar). For (B), (C), and (F–H), data are representative of average ± SD of three independent experiments. *$p < 0.05$, **$p < 0.005$. See also Figure S4.

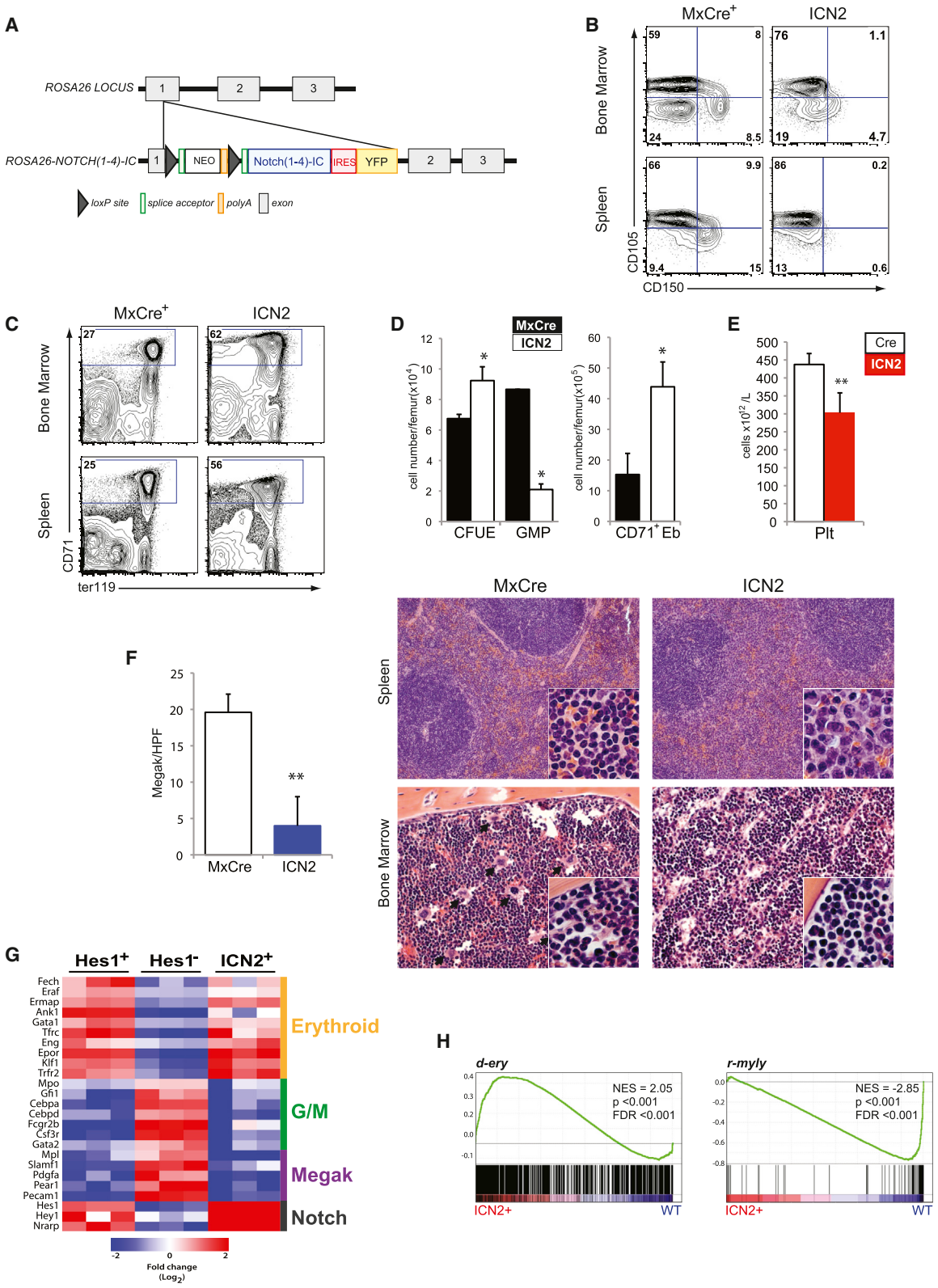

Figure 5. Notch2 Gain of Function Enhances Erythroid Differentiation

(A) Generation of ROSA26-Notch(1–4)-IC mice for conditional expression of intracellular Notch and IRES-YFP driven by the ROSA26 promoter.

(B) Representative FACS plot of erythroid progenitors. CFU-E progenitors were increased in both the spleen and bone marrow upon conditional expression of ICN2.

(legend continued on next page)

consequences of expressing each of the four ICNs from the same promoter in hematopoiesis. Interestingly, although we could demonstrate that all transgenes were expressed at comparable levels (Figure S5A and not shown), only expression of ICN1 was sufficient to induce T cell leukemia in vivo (Figure S5B), suggesting that each ICN defines distinct thresholds of signaling strength. Because Notch2 is the only receptor expressed during early erythropoiesis, we focused our subsequent gain-of-function studies on the effect of Notch2 activation (ICN2) in bone marrow hematopoietic progenitors. Activation of ICN2 expression in hematopoietic cells using the polyI:polyC inducible Mx1-Cre resulted in a significant increase of $CD105^+$ CFU-E erythroid progenitors and $CD71^+$ erythroblasts in the bone marrow and spleen (Figures 5B–5D). Platelet counts were significantly reduced in mice when ICN2 was expressed (Figure 5E and Table S1). Histological analysis (Figure 5F) showed that a dramatic increase in nucleated cells was apparent in the splenic red pulp at low power, and the margins of B cell follicles appeared to be blurred. ICN2 nucleated cells clearly displayed the morphology of erythroid blast cells. Numerous early erythroid progenitors and erythroblasts were abundant. In the bone marrow, there was an increase in erythroid progenitor cells, which was also confirmed by staining and differential counts of bone marrow smears (data not shown). Strikingly, there was 5-fold reduction of Mks in ICN2 bone marrow (Figure 5F), in agreement with the suggested negative role of the Notch pathway in megakaryopoiesis.

We next sought to examine gene expression of sorted $cKit^+$ progenitors that express activated ICN2 in vivo. As seen in *Hes1*$^+$ progenitors, ICN2-expressing progenitors upregulated erythroid genes and suppressed GM and Mk genes (Figure 5G). Transcriptional targets of Notch were upregulated in ICN2-expressing progenitors, confirming the ICN2 functionality. As with *Hes1*-expressing $cKit^+$ progenitors and pre-MegEs, the expression of erythroid gene sets (*d-ery*) was enriched, while the expression of genes expressed in lymphoid or GM progenitors (*r-myly*) was suppressed (Ng et al., 2009) (Figure 5H). To further address the involvement of Notch in the choice between the erythroid and Mk lineages, we imposed the expression of ICN2 in liquid cultures of $cKit^+$ progenitors using a $ROSA26^{CreER}$ driver and 4-hydroxytamoxifen (4-OHT). In the ROSA26-YFP control, after being inducted with 4-OHT, both $CD71^+$ erythroblasts and Mks were generated in culture. However, induction of ICN2 expression directed the differentiation of the progenitors into mostly $CD71^+$ erythroblasts and inhibited the generation of $FSC^{high}CD41^+$ Mks (Figure S5C). These combined studies further support our main hypothesis in that they demonstrated that Notch2 gain of function enforces erythrocytic commitment both in vitro and in vivo.

Notch Loss of Function Inhibits Early Erythroid Progenitor Differentiation

To study effects of Notch loss of function, we used either deletion of *Notch1* and *Notch2* or *Nicastrin* (a nonredundant part of the γ-secretase complex) to avoid putative compensatory receptor functions (Klinakis et al., 2011). We conditionally deleted Notch signaling in adult mice using the *Mx1-Cre* deleter strain and analyzed bone marrow progenitor distribution, focusing on erythroblasts. In agreement with previous reports, no overt anemia under steady-state conditions was noticed (Maillard et al., 2008; Mancini et al., 2005). However, in the absence of Notch signaling, we found that both the frequency and absolute numbers of $CD105^+$ CFU-E progenitors and $CD45^-CD71^+$ erythroblasts were significantly reduced in comparison to those of control mice (Figures 6A–6C). Furthermore, CFU-E and CFU-Mk assays using flow-purified $Lin^{neg}/cKit^+/Sca1^-$ progenitors showed a decreased ability of Notch-deficient progenitors to generate CFU-Es and an increased ability of such to generate CFU-Mks (Figure S6A). In contrast to the aforementioned gain-of-function analysis using ICN2 ectopic expression, Notch loss of function (in both $Notch1^{-/-}2^{-/-}$ and $Ncstn^{-/-}$ mice) lead to increased platelet counts and numbers of splenic Mks (Figure 6D, Figure S6B). Cell cycle and apoptosis analysis of pre-MegE, pre-CFU-E, and CFU-E populations revealed no significant differences between $Ncstn^{-/-}$ and littermate controls (Figures S6C and S6D), suggesting that the reduction of the CFU-E population observed in Notch loss-of-function models is mainly due to differentiation bias. These data are consistent with our previous in vitro and in vivo studies, enforcing the idea that in a subset of progenitors, Notch signaling is important for early stages of lineage commitment and erythroid progenitor differentiation.

Notch Signaling Is Essential for Optimal Progenitor Responses during Stress Erythropoiesis

To further test the importance of Notch signaling for the generation of adult red blood cells (RBCs) and their progenitors, we deleted *Ncstn* specifically in the hematopoietic system using *Vav1-cre*$^+$ *Ncstn*$^{f/f}$ animals and studied the response to stress caused initially by the administration of phenylhydrazine (PHZ), an oxidative agent able to cause severe hemolytic anemia. Whereas no significant difference in the peripheral blood red cell compartment was observed at steady state (Figure S6B), *Ncstn*-deficient animals showed a significant delay of recovery from stress as demonstrated by lower numbers of total RBCs (Figure 6E) circulating in the peripheral blood. Because PHZ mainly targets mature RBCs and we have shown that the activation of the Notch pathway is only transient and not evident in the later stages of RBC differentiation, we focused on an additional

(C) Representative FACS plot of erythroblasts. $CD71^+$ erythroblasts were increased in the spleen and bone marrow with ICN2.
(D) Bar graph showing absolute myelo-erythroid progenitor counts per femur (n = 4).
(E) Platelet counts from peripheral blood of WT (white bar), $ICN1^+$ (blue bar), or $ICN2^+$ (red bar) mice.
(F) H&E-stained sections of spleen and bone marrow from control and ICN2 mice. Images are at 10× magnification with 63× magnification inset in lower right. Bone marrow megakaryocytes were counted in five bone marrow (10×) high-powered fields (HPFs) (n = 3). For (D)–(F), data are representative of mean ± SD. *$p < 0.05$, **$p < 0.005$.
(G) $Lin^{neg}/cKit^{+/}Sca1^-$ progenitors expressing ICN2 were sorted for gene expression arrays and a heat map of genes involved in lineage specific differentiation was generated.
(H) GSEA of erythroid gene signatures (*d-ery*) and myeloid-lymphoid genes (*r-myly*) in $ICN2^+$ versus WT littermates $Lin^{neg}/cKit^{+/}Sca1^-$ progenitors.
See also Figure S5 and Table S1.

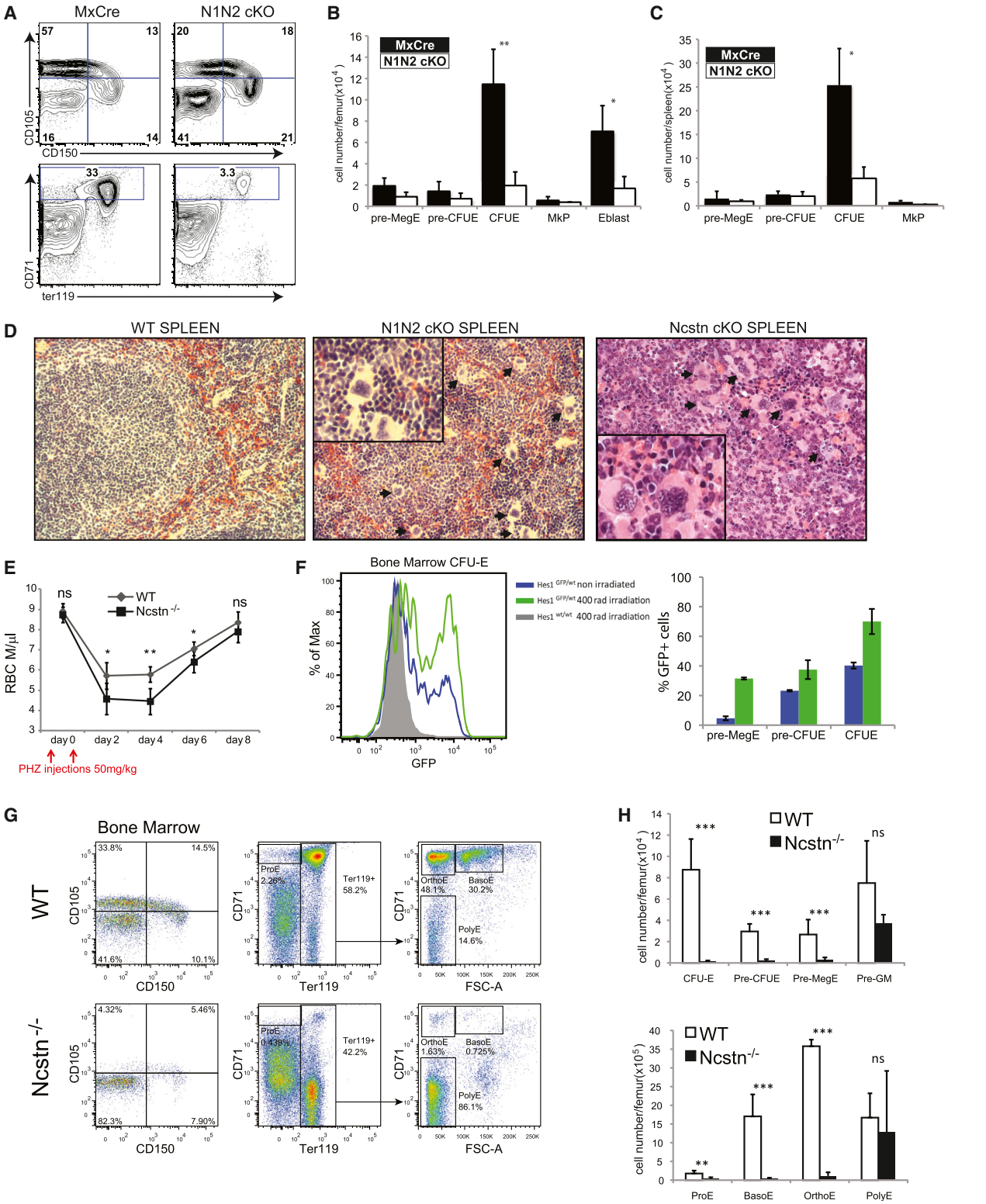

Figure 6. Notch Loss of Function Affects Early Erythroid Differentiation and Recovery from Erythroid Stress

(A) Adult mice were analyzed 1 week after three injections of polyI:polyC to induce compound deletion of *Notch1* and *Notch2* using the *Mx1-Cre* strain (*Mx1cre*$^{+}$*Notch1*$^{-/-}$*2*$^{-/-}$). The frequency of CFU-E progenitors and CD45^{-}CD71^{+} erythroblasts is shown.

(B and C) Absolute numbers of early erythroid progenitors in control and *Notch1*$^{-/-}$*2*$^{-/-}$ mice (n = 5) from (B) bone marrow and (C) spleen. Data represent mean ± SD.

(legend continued on next page)

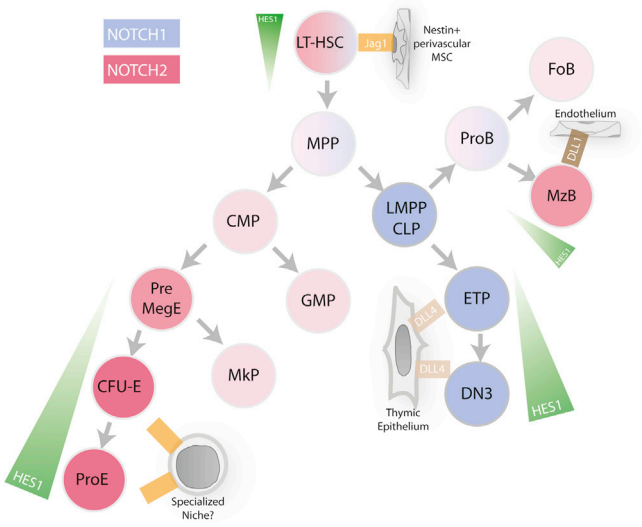

Figure 7. "Road Map" of Notch Signaling Pathway in Hematopoiesis
General overview of level of Notch1 receptor expression (blue gradient), Notch2 receptor expression (red gradient), Notch signaling pathway activation reported by $Hes1^{GFP}$ expression (green gradient), and known niches and Notch ligands involved in adult hematopoiesis. LT-HSC, long-term hematopoietic stem cell; MPP, multipotential progenitor; CMP, common myeloid progenitor; GMP, granulocyte-monocyte progenitor; pre-MegE, pre-megakaryocyte/erythrocyte progenitor; MkP, megakaryocyte progenitor; CFU-E, colony forming unit erythrocyte; ProE, proerythroblast; LMPP, lymphocyte-primed multipotential progenitor; CLP, common lymphocyte progenitor; ProB, pro B cell; FoB, follicular B cell; MzB, marginal zone B cell; ETP, Early thymic progenitor; DN, double negative ($CD4^-8^-$) T cell progenitor 3.

stress stimulus. We selected sublethal ionizing radiation, which rapidly eliminates marrow and splenic erythroid progenitors while sparing mature peripheral RBCs (Peslak et al., 2012). Using this stress stimulus we initially demonstrated that irradiation significantly increased the abundance of $Hes1^{GFP}$ erythrocytic progenitors (Figure 6F) in the bone marrow, a response initiated as early as the pre-MegE stage. Interestingly, Notch2 receptor cell surface expression was increased in pre-MegE cells in response to stress (Figure S6D). These studies suggested an enhanced activation of the Notch pathway in response to erythrocytic stress. Most importantly, irradiation of $Ncstn^{-/-}$ animals revealed their profound inability to mount a response to radiation-induced erythroid stress in the absence of Notch signaling. Indeed, both early (CFU-E, pre-CFU-E, and pre-MegE) and late (ProE, Basophilic Erythrocyte [BasoE], and Orthochromatic Erythrocyte [OrthoE]) stages of RBC differentiation were virtually absent in mice lacking Notch signaling (Figures 6G and 6H). On the other hand, recovery of the pre-GM population was not significantly altered in $Ncstn^{-/-}$, suggesting that the defects are specific to the erythroid lineage.

Because Notch2 is the only Notch receptor expressed on the surface of erythrocytic progenitors, we have also tested whether *Notch2* deficiency is sufficient to impede differentiation of erythrocyte progenitors in response to stress. To exclude contributions from the microenvironment, we have transplanted $Vav1\text{-}cre^{+}Notch2^{f/f}CD45.2^{+}$ bone marrow into irradiated congenic $CD45.1^{+}$ recipients. As a control we have used $Vav1\text{-}cre^{-}Notch2^{f/f}CD45.2^{+}$ bone marrow from littermate animals. Five weeks posttransplant and after we verified that recipient animal bone marrow comprised more than 90% of $Notch2^{neg}$ donor cells (Figures S7A and S7B), we sublethaly irradiated the animals and analyzed erythrocytic stress response as previously described. Four days postirradiation $Vav1\text{-}cre^{+}Notch2^{f/f}$ reconstituted animals showed signs of defective stress response, including smaller spleens and significantly decreased numbers of pre-CFU-E and CFU-E progenitors (Figures S7C–S7E) in the spleen. On the other hand there were no significant differences in the recovery of GM and Mk progenitors, suggesting specificity for the erythrocytic lineage. All these studies highlight the importance of Notch signaling, and specifically Notch2, in stress erythropoiesis.

DISCUSSION

Our lineage tracing experiments provide a window into the mechanisms utilized by distinct Notch receptors in adult and fetal hematopoiesis. They offer in vivo mapping of receptor expression and activity in the bone marrow and extramedullary sites (Figure 7). Indeed, they identify a remarkable division of labor between Notch receptors, connecting *Notch1* expression to commitment to the lymphoid lineage and *Notch2* expression to the initiation of erythrocytic differentiation. On the other hand, *Notch3* and *Notch4* were not associated with bone marrow stem/progenitor cells. Although CreER-mediated target loci deletion is expression level dependent and recombination may not occur at low levels of gene expression, our studies strongly suggest that *Notch1* and *Notch2* are the main regulators of early adult hematopoiesis. In agreement with this notion and our lineage tracing findings, antibody staining for Notch1 and Notch2 in progenitors further confirmed our genetic fate mapping. Furthermore, quantitative RT-PCR analysis and antibody staining for Notch4 confirmed the results obtained with the lineage tracing, beacuse mRNA and cell surface expression of this receptor were undetectable in all bone marrow stem and progenitor subsets. Finally, in vivo reporter activity together with loss- and gain-of-function genetic studies demonstrated the crucial role for Notch signaling in early stages of hematopoietic differentiation and stress erythropoiesis. This demonstrates the role of Notch in RBC differentiation in vivo. It is noteworthy that meta-analysis of human progenitor gene expression data sets demonstrated that Notch activity is also increased when human

(D) H&E-stained paraffin sections of spleens from control, $Notch1^{-/-}2^{-/-}$, and $Ncstn^{-/-}$ mice. Megakaryocytes are indicated with black arrows.
(E) Erythropoietic response to acute hemolytic anemia in control ($Ncstn^{f/f}$) and $Ncstn^{-/-}$ ($Vav1\text{-}cre\ Ncstn^{f/f\ +}$) (n = 5) after PHZ-induced hemolysis. Data represent mean ± SD.
(F) Representative FACS plot (left panel) and quantification of proportion of GFP^{+} cells in $Hes1^{GFP/wt}$ mice before (blue) and 4 days after (green) sublethal 4Gy irradiation. Data represent mean ± SD of three biological replicates.
(G and H) Representative FACS plots (G) and absolute quantification (H) of erythroid progenitors from bone marrow of control ($Ncstn^{f/f}$) and $Ncstn^{-/-}$ ($Vav1\text{-}cre^{+}$ $Ncstn^{f/f}$) (n = 3) littermates 4 days after sublethal 4Gy irradiation. Data represent mean ± SD. *p < 0.05, **p < 0.005, ***p < 0.001.
See also Figures S6 and S7.

stem and progenitor cells commit to the erythroid lineage, suggesting that the involvement of Notch signaling during erythropoiesis is evolutionary conserved. Finally, we were able to show that Notch-dependent regulation of erythropoiesis occurs only in adult hematopoiesis and is crucial for efficient recovery from erythrocytic stress and life-threatening anemia induced by exposure to ionizing irradiation or blood loss.

Our studies also provide insights into the role of Notch signaling in the differentiation of adult HSCs. We were able to clearly identify Notch receptors that are expressed on LT-HSCs, mainly Notch2, and show that the transcriptional target *Hes1* is activated in a subset of HSCs under homeostatic conditions. Purification and subsequent serial transplantations of *Notch2*$^{RFP+}$ and *Hes1*$^{GFP+}$ LSKs demonstrated that they contain bona fide HSCs (not shown). In agreement with this notion, analysis of sorted *Hes1*$^{GFP+}$ LSKs reveals molecular correlation to HSC gene expression signatures. However, we were also able to show that *Hes1*$^{GFP+}$ LSK cells have a molecular priming toward the erythrocytic lineage using in vitro assays and transcriptome analysis. This differentiation bias toward the erythrocytic lineage becomes even more apparent at subsequent stages of differentiation: multipotent Lin^{neg}cKit^{+} or bipotent pre-MegE progenitors expressing *Hes1*^{GFP} have a propensity to differentiate into erythrocytes and are characterized by erythrocytic gene signatures. On the other hand, without Notch activation, progenitors (*Hes1*^{GFP} negative) mainly differentiate toward the GM or Mk lineages. There are significant consequences of these findings, because they suggest that Notch signaling could have distinct roles in different blood lineages. In agreement with this notion, it was shown that Notch could turn from an oncogene (T cell leukemia, B cell lymphoma) (Grabher et al., 2006; Puente et al., 2011) to a tumor suppressor (myelo-monocytic leukemia) (Klinakis et al., 2011) depending on the type of hematopoietic progenitor initiating each disease. Our current studies would suggest that in addition to Notch inhibition, receptor-specific pathway agonism could also be a promising therapeutic alternative in tumors characterized by silencing of the pathway (Lobry et al., 2011, 2013).

It would be intriguing to integrate our findings with previously published reports on Notch function in early hematopoiesis. The discovery of a role for Notch signaling in erythrocytic differentiation and stress response could open clinically important areas of future investigation. We clearly show that Notch signaling suppresses Mk differentiation, which is in agreement with its role in the promotion of erythropoiesis but is inconsistent with a previous report suggesting that Notch4 can promote differentiation toward this lineage (Mercher et al., 2008). However, those studies were based largely on in vitro cultures performed in the presence of transfected Notch ligands and exogenous Thrombopoietin. Nevertheless, our findings are in agreement with a recent in vitro study focusing on human hematopoiesis and suggesting a negative role for the Notch pathway in megakaryopoiesis (Poirault-Chassac et al., 2010). Although it is difficult to reconcile all these studies, it is possible that they are all correct, because at different stages of differentiation Notch signaling could have distinct effects on MEP commitment/maintenance or even mature Mk differentiation and maturation.

Our data also suggest the existence of progenitor cell niches characterized by Notch ligand expression (Figure 7) responsible for commitment to distinct cell fates. Indeed, our work suggests that in the bone marrow there are distinct Notch ligand-expressing niches, responsible for HSC function as well as lymphocytic and erythrocytic differentiation. Although it would be intriguing to correlate Notch signaling to specific ligand microenvironments, development of in vivo genetic reporters in combination with advanced imaging is required to further characterize and analyze specific ligand expression and role. Furthermore, our finding that activation of Notch2-mediated signaling stimulates erythroid differentiation and is essential in the response to erythrocytic stress could also be clinically important. Anemia is a common feature of patients with renal disease and chronic heart failure and occurs in the majority of cancer patients (Melnikova, 2006). Currently, recombinant EPO is used to treat anemia and provides significant clinical benefit (Eschbach et al., 1987). However, resistance to EPO treatment or an insufficiency of erythroid progenitors is found in many patients (van der Putten et al., 2008). It is possible that such patients will benefit from simultaneous activation of Notch2 and EPO receptors. Bioavailable peptide ligands or specific Notch2 receptor agonists could thus be important in such clinical settings.

EXPERIMENTAL PROCEDURES

Animals

Notch(1–4)^{CreER} and *Hes1*^{GFP} knockin mice were recently described (Fre et al., 2011). *ROSA26*$^{ICN(1–4)}$ mice were generated by inserting a loxP flanked splice acceptor NEO-ATG cassette with two polyA sites followed by ICN(1–4)-IRES-YFP into the ROSA26 locus, allowing the ROSA26 promoter to drive expression of the NEO-ATG cassette. Cre-recombinase-mediated excision of NEO-ATG results in use of the splice acceptor in the ICN(1–4)-IRES-YFP cassette and irreversible expression of the transgene, and the IRES-YFP bicistronic mRNA allows expression to be monitored by YFP expression. *ROSA26*^{lslRFP} mice (gift from H.-J. Fehling, Ulm University) and *ROSA26*^{lslYFP} animals (gift from D. Littman, NYU School of Medicine) have been described (Luche et al., 2007; Srinivas et al., 2001). Inducible Cre animals used include the following: the tamoxifen inducible human ubiquitin C promoter driven CreER (*Ubc-CreER*) (Ruzankina et al., 2007) (gift from D. Littman, NYU School of Medicine), tamoxifen inducible ROSA26^{CreER} (Seibler et al., 2003) (gift from D. Littman, NYU School of Medicine), and polyI:polyC inducible *Mx1-Cre* (Jackson Labs). *Notch1*$^{f/f}$ *Notch2*$^{f/f}$ and *Ncstn*$^{f/f}$ mice were previously described (Klinakis et al., 2011). Hematopoietic specifique *Vav1-cre* was previously described (Stadtfeld and Graf, 2005). All animal experiments were done in accordance with the guidelines of the NYU School of Medicine Institutional Animal Care and Use Committee.

Notch Lineage Tracing and LSK Transplants

Tamoxifen (Sigma Aldrich) was solubilized in corn oil (Sigma Aldrich) at a concentration of 20 mg/ml and injected intraperitoneally at 0.2 mg/g body weight. Following (1 or 3) daily injections and a 3 day, 7 day, or 20 week chase, animals were euthanized for analysis of peripheral blood and tissues by FACS. For transplantation of RFP-labeled LSK cells, *ROSA26*^{CreER}, *Notch1*^{CreER}, and *Notch2*^{CreER} lineage tracer mice were crossed to *ROSA26*^{lslRFP} reporter mice and injected with tamoxifen daily for 3 days (0.2 mg/g mouse). Two days after the last injection, bone marrow was isolated from femurs and tibias. Lineage-depleted cells were stained as described, RFP^{+} LSK cells were sorted, and 500–750 cells were transplanted with 2.5 × 10^{5} helper bone marrow cells into lethally irradiated recipients. Peripheral blood was analyzed 4 weeks and 24 weeks posttransplant.

Stress Erythropoiesis

PHZ was dissolved in PBS and injected intraperitoneally at 50 mg/kg on two consecutive days to induce acute anemia. Peripheral blood (50 μl) was collected and analyzed using the Hemavet 950 (Drew Scientific) hematology

system. Sublethal total body irradiation of 4 Gy radiation was used to model endogenous stress erythropoiesis as previously described (Peslak et al., 2012). Progenitor responses were analyzed at day 4 following sublethal irradiation.

Antibodies and Flow Cytometry

Freshly dissected femurs and tibias were dissected and bone marrow was flushed with a 3 cm^3 syringe and 25G needle into PBS with 3% FBS. The bone marrow suspension was centrifuged at 400 rcf for 10 min at 4°C, washed, and resuspended in PBS with 3% FBS. Antibody staining and FACS analysis was performed as previously described (Klinakis et al., 2011). All antibodies were purchased from BD-PharMingen or e-Bioscience. We used the following fluorochrome or biotin conjugated antibodies: CD117 (2B8), Sca-1 (D7), CD11b (M1/70), Gr-1 (RB6-8C5), NK1.1 (PK136), TER-119, CD3 (145-2C11), CD19 (1D3), CD21 (7E9), CD23 (B3B4), CD127 (A7R34), CD34 (RAM34), FcγRII/III (2.4G2 or 93), CD135 (A2F10.1), CD4 (RM4-5), CD8 (53-6.7), CD150 (9D1), CD41 (MWReg30), B220 (RA3-6B2), CD48 (HM481), CD105 (MJ7/18), F4/80 (BM8), and CD71 (RI7217). Bone marrow lineage antibody cocktail included CD11b, Gr-1, NK1.1, TER-119, CD4, CD8, CD3, B220, and Il7Rα. For analysis of erythroid progenitors, TER-119 was not included in lineage cocktail as previously described (Pronk et al., 2007).

Microarray and GSEA

Human hematopoietic population microarray data have been previously described (Novershtern et al., 2011) and are available at the GEO database (http://www.ncbi.nlm.nih.gov/geo/) under accession number GSE24759. Data were normalized using the Robust Multi-array Average algorithm using Genespring GX software (Agilent) and gene expressions were leveled according to GAPDH expression. Mouse erythoid and myeloid progenitor population microarrays have been previously described (Pronk et al., 2007) and are available at GEO database under accession number GSE8407.

Microarray analysis was performed as previously described (Klinakis et al., 2011). For each experiment, freshly isolated cells from three individual mice were sorted by surface marker expression and GFP expression and total RNA was extracted using the RNeasy Plus Micro kit (QIAGEN). The Ovation RNA Amplification System V2 or Ovation Pico amplification (NuGEN) kits were used for amplification. Amplified RNA was labeled and hybridized to the Mouse 430.2 microarrays (Affymetrix). The Affymetrix gene expression profiling data were normalized using the previously published robust multiarray average algorithm using the GeneSpring GX software (Agilent). The gene-expression intensity presentations were generated with Multi Experiment Viewer software (http://www.tm4.org/mev/). GSEA was performed using GSEA software (http://www.broadinstitute.org/gsea) using gene set as permutation type, 1,000 permutations, and $\log_2$ ratio of classes as metric for ranking genes. Gene sets used in this study have been previously published (Mercher et al., 2008; Ng et al., 2009; Pronk et al., 2007).

In Vitro Differentiation Assays

Sorted LSKs, $Lin^{neg}/cKit^{+}/Sca1^{-}$ progenitors (500), or pre-MegEs (500) were plated in triplicate into cytokine-supplemented methylcellulose medium (MethoCult 3434, Stem Cell Technologies). Colonies were scored after 10 days of culture and cells were collected for analysis by FACS. For CFU-E assays cells were plated in methylcellulose medium supplemented with EPO (MethoCult 3334, Stem Cell Technologies) and colonies were counted 2 days after plating. Collagen gel assays for CFU-Mks were performed using Megacult-C (supplemented TPO and IL-3, Peprotech). Collagen gels were acetone fixed and AchE staining was performed according to the manufacturer's guidelines (MegaCult-C, Stem Cell Technologies).

Statistical Analysis

The means of each data set were analyzed using Student's t test with a two-tailed distribution and assuming equal sample variance.

ACCESSION NUMBERS

Newly generated microarray data are available at GEO database under accession number GSE46726.

SUPPLEMENTAL INFORMATION

Supplemental Information for this article includes Supplemental Experimental Procedures, seven figures, and one table and can be found with this article online at http://dx.doi.org/10.1016/j.stem.2013.05.015.

ACKNOWLEDGMENTS

We are grateful to H.-J. Fehling for the ROSA26-RFP mice and Linheng Li, Paul Frenette, and Amy Wagers for sharing experimental tools and advice. We would like to thank the NYU Genome Technology Center (supported in part by NIH/NCI P30 CA016087-30 grant) for expert assistance with microarray experiments; the NYU Flow Cytometry facility (supported in part by NIH/NCI 5 P30CA16087-31) for expert cell sorting; the NYU Histology Core (5P30CA16087-31); the Transgenic Mouse Core (NYU Cancer Institute Center Grant (5P30CA16087-31); and Jacquelyn Freund for technical assistance. I.A. is supported by the National Institutes of Health (RO1CA133379, RO1CA105129, RO1CA149655, and RO1GM088847), the Leukemia & Lymphoma Society (TRP program grants), The V Foundation for Cancer Research, the Irma T. Hirschl Trust, and the St. Baldrick's Foundation for Cancer Research. P.O. was supported by the NYU MSTP Program. C.L. was supported by the Helen and Martin Kimmel Center for Stem Cell Research and is currently a Leukemia and Lymphoma Society Fellow. The research in the S.A.-T. laboratory was supported by the NIH (RO1 CA 098402). I.A. is a Howard Hughes Medical Institute Early Career Scientist. *Hes1*^{GFP} and *Notch(1–4)*^{CreER} mice are available upon request to Dr. Artavanis-Tsakonas.

Received: January 2, 2013
Revised: May 2, 2013
Accepted: May 17, 2013
Published: June 20, 2013

REFERENCES

Artavanis-Tsakonas, S., Matsuno, K., and Fortini, M.E. (1995). Notch signaling. Science *268*, 225–232.

Butler, J.M., Nolan, D.J., Vertes, E.L., Varnum-Finney, B., Kobayashi, H., Hooper, A.T., Seandel, M., Shido, K., White, I.A., Kobayashi, M., et al. (2010). Endothelial cells are essential for the self-renewal and repopulation of Notch-dependent hematopoietic stem cells. Cell Stem Cell *6*, 251–264.

Ciofani, M., and Zúñiga-Pflücker, J.C. (2005). Notch promotes survival of pre-T cells at the β-selection checkpoint by regulating cellular metabolism. Nat. Immunol. *6*, 881–888.

Clements, W.K., Kim, A.D., Ong, K.G., Moore, J.C., Lawson, N.D., and Traver, D. (2011). A somitic Wnt16/Notch pathway specifies haematopoietic stem cells. Nature *474*, 220–224.

Dzierzak, E., and Speck, N.A. (2008). Of lineage and legacy: the development of mammalian hematopoietic stem cells. Nat. Immunol. *9*, 129–136.

Eschbach, J.W., Egrie, J.C., Downing, M.R., Browne, J.K., and Adamson, J.W. (1987). Correction of the anemia of end-stage renal disease with recombinant human erythropoietin. Results of a combined phase I and II clinical trial. N. Engl. J. Med. *316*, 73–78.

Fiorini, E., Merck, E., Wilson, A., Ferrero, I., Jiang, W., Koch, U., Auderset, F., Laurenti, E., Tacchini-Cottier, F., Pierres, M., et al. (2009). Dynamic regulation of notch 1 and notch 2 surface expression during T cell development and activation revealed by novel monoclonal antibodies. J. Immunol. *183*, 7212–7222.

Fre, S., Hannezo, E., Sale, S., Huyghe, M., Lafkas, D., Kissel, H., Louvi, A., Greve, J., Louvard, D., and Artavanis-Tsakonas, S. (2011). Notch lineages and activity in intestinal stem cells determined by a new set of knock-in mice. PLoS ONE *6*, e25785.

Grabher, C., von Boehmer, H., and Look, A.T. (2006). Notch 1 activation in the molecular pathogenesis of T-cell acute lymphoblastic leukaemia. Nat. Rev. Cancer *6*, 347–359.

Hirata, H., Yoshiura, S., Ohtsuka, T., Bessho, Y., Harada, T., Yoshikawa, K., and Kageyama, R. (2002). Oscillatory expression of the bHLH factor Hes1 regulated by a negative feedback loop. Science *298*, 840–843.

Jackson, C.W. (1973). Cholinesterase as a possible marker for early cells of the megakaryocytic series. Blood *42*, 413–421.

Kleinmann, E., Geimer Le Lay, A.-S., Sellars, M., Kastner, P., and Chan, S. (2008). Ikaros represses the transcriptional response to Notch signaling in T-cell development. Mol. Cell. Biol. *28*, 7465–7475.

Klinakis, A., Lobry, C., Abdel-Wahab, O., Oh, P., Haeno, H., Buonamici, S., van De Walle, I., Cathelin, S., Trimarchi, T., Araldi, E., et al. (2011). A novel tumour-suppressor function for the Notch pathway in myeloid leukaemia. Nature *473*, 230–233.

Kopan, R., and Ilagan, M.X. (2009). The canonical Notch signaling pathway: unfolding the activation mechanism. Cell *137*, 216–233.

Kühn, R., Schwenk, F., Aguet, M., and Rajewsky, K. (1995). Inducible gene targeting in mice. Science *269*, 1427–1429.

Kumano, K., Chiba, S., Kunisato, A., Sata, M., Saito, T., Nakagami-Yamaguchi, E., Yamaguchi, T., Masuda, S., Shimizu, K., Takahashi, T., et al. (2003). Notch1 but not Notch2 is essential for generating hematopoietic stem cells from endothelial cells. Immunity *18*, 699–711.

Lobry, C., Oh, P., and Aifantis, I. (2011). Oncogenic and tumor suppressor functions of Notch in cancer: it's NOTCH what you think. J. Exp. Med. *208*, 1931–1935.

Lobry, C., Ntziachristos, P., Ndiaye-Lobry, D., Oh, P., Cimmino, L., Zhu, N., Araldi, E., Hu, W., Freund, J., Abdel-Wahab, O., et al. (2013). Notch pathway activation targets AML-initiating cell homeostasis and differentiation. J. Exp. Med. *210*, 301–319.

Luche, H., Weber, O., Nageswara Rao, T., Blum, C., and Fehling, H.J. (2007). Faithful activation of an extra-bright red fluorescent protein in "knock-in" Cre-reporter mice ideally suited for lineage tracing studies. Eur. J Immunol. 43–53.

Maillard, I., Koch, U., Dumortier, A., Shestova, O., Xu, L., Sai, H., Pross, S.E., Aster, J.C., Bhandoola, A., Radtke, F., and Pear, W.S. (2008). Canonical notch signaling is dispensable for the maintenance of adult hematopoietic stem cells. Cell Stem Cell *2*, 356–366.

Mancini, S.J.C., Mantei, N., Dumortier, A., Suter, U., MacDonald, H.R., and Radtke, F. (2005). Jagged1-dependent Notch signaling is dispensable for hematopoietic stem cell self-renewal and differentiation. Blood *105*, 2340–2342.

Melnikova, I. (2006). Anaemia therapies. Nat. Rev. Drug Discov. *5*, 627–628.

Mercher, T., Cornejo, M.G., Sears, C., Kindler, T., Moore, S.A., Maillard, I., Pear, W.S., Aster, J.C., and Gilliland, D.G. (2008). Notch signaling specifies megakaryocyte development from hematopoietic stem cells. Cell Stem Cell *3*, 314–326.

Moriyama, Y., Sekine, C., Koyanagi, A., Koyama, N., Ogata, H., Chiba, S., Hirose, S., Okumura, K., and Yagita, H. (2008). Delta-like 1 is essential for the maintenance of marginal zone B cells in normal mice but not in autoimmune mice. Int. Immunol. *20*, 763–773.

Ng, S.Y.-M., Yoshida, T., Zhang, J., and Georgopoulos, K. (2009). Genome-wide lineage-specific transcriptional networks underscore Ikaros-dependent lymphoid priming in hematopoietic stem cells. Immunity *30*, 493–507.

Novershtern, N., Subramanian, A., Lawton, L.N., Mak, R.H., Haining, W.N., McConkey, M.E., Habib, N., Yosef, N., Chang, C.Y., Shay, T., et al. (2011). Densely interconnected transcriptional circuits control cell states in human hematopoiesis. Cell *144*, 296–309.

Ntziachristos, P., Tsirigos, A., Van Vlierberghe, P., Nedjic, J., Trimarchi, T., Flaherty, M.S., Ferres-Marco, D., da Ros, V., Tang, Z., Siegle, J., et al. (2012). Genetic inactivation of the polycomb repressive complex 2 in T cell acute lymphoblastic leukemia. Nat. Med. *18*, 298–301.

Orkin, S.H., and Zon, L.I. (2008). Hematopoiesis: an evolving paradigm for stem cell biology. Cell *132*, 631–644.

Peslak, S.A., Wenger, J., Bemis, J.C., Kingsley, P.D., Koniski, A.D., McGrath, K.E., and Palis, J. (2012). EPO-mediated expansion of late-stage erythroid progenitors in the bone marrow initiates recovery from sublethal radiation stress. Blood *120*, 2501–2511.

Poirault-Chassac, S., Six, E., Catelain, C., Lavergne, M., Villeval, J.L., Vainchenker, W., and Lauret, E. (2010). Notch/Delta4 signaling inhibits human megakaryocytic terminal differentiation. Blood *116*, 5670–5678.

Pronk, C.J.H., Rossi, D.J., Månsson, R., Attema, J.L., Norddahl, G.L., Chan, C.K.F., Sigvardsson, M., Weissman, I.L., and Bryder, D. (2007). Elucidation of the phenotypic, functional, and molecular topography of a myeloerythroid progenitor cell hierarchy. Cell Stem Cell *1*, 428–442.

Puente, X.S., Pinyol, M., Quesada, V., Conde, L., Ordóñez, G.R., Villamor, N., Escaramis, G., Jares, P., Beà, S., González-Díaz, M., et al. (2011). Whole-genome sequencing identifies recurrent mutations in chronic lymphocytic leukaemia. Nature *475*, 101–105.

Ruzankina, Y., Pinzon-Guzman, C., Asare, A., Ong, T., Pontano, L., Cotsarelis, G., Zediak, V.P., Velez, M., Bhandoola, A., and Brown, E.J. (2007). Deletion of the developmentally essential gene ATR in adult mice leads to age-related phenotypes and stem cell loss. Cell Stem Cell *1*, 113–126.

Seibler, J., Zevnik, B., Küter-Luks, B., Andreas, S., Kern, H., Hennek, T., Rode, A., Heimann, C., Faust, N., Kauselmann, G., et al. (2003). Rapid generation of inducible mouse mutants. Nucleic Acids Res. *31*, e12.

Sekine, C., Moriyama, Y., Koyanagi, A., Koyama, N., Ogata, H., Okumura, K., and Yagita, H. (2009). Differential regulation of splenic CD8- dendritic cells and marginal zone B cells by Notch ligands. Int. Immunol. *21*, 295–301.

Srinivas, S., Watanabe, T., Lin, C.S., William, C.M., Tanabe, Y., Jessell, T.M., and Costantini, F. (2001). Cre reporter strains produced by targeted insertion of EYFP and ECFP into the ROSA26 locus. BMC Dev. Biol. *1*, 4.

Stadtfeld, M., and Graf, T. (2005). Assessing the role of hematopoietic plasticity for endothelial and hepatocyte development by non-invasive lineage tracing. Development *132*, 203–213.

Tanigaki, K., Han, H., Yamamoto, N., Tashiro, K., Ikegawa, M., Kuroda, K., Suzuki, A., Nakano, T., and Honjo, T. (2002). Notch-RBP-J signaling is involved in cell fate determination of marginal zone B cells. Nat. Immunol. *3*, 443–450.

van der Putten, K., Braam, B., Jie, K.E., and Gaillard, C.A. (2008). Mechanisms of Disease: erythropoietin resistance in patients with both heart and kidney failure. Nat. Clin. Pract. Nephrol. *4*, 47–57.

Varnum-Finney, B., Halasz, L.M., Sun, M., Gridley, T., Radtke, F., and Bernstein, I.D. (2011). Notch2 governs the rate of generation of mouse long- and short-term repopulating stem cells. J. Clin. Invest. *121*, 1207–1216.